Pharmacology Biochemistry & Behavior, Vol. 40, pp. 547–552. © Pergamon Press plc, 1991. Printed in the U.S.A. 0091-3057/91 $3.00 + .00

Small Angle X-Ray Diffraction Studies on the Topography of Cannabinoids in Synaptic Plasma Membranes

THOMAS MAVROMOUSTAKOS,* DE-PING YANG,*[1] WANDA BRODERICK,* DONNA FOURNIER* AND ALEXANDROS MAKRIYANNIS*†‡

**School of Pharmacy and Institute of Materials Science, University of Connecticut, Storrs, CT 06269*
†Biomolecular Structure Analysis Center, University of Connecticut Health Center, Farmington, CT 06032
‡Francis Bitter National Magnet Laboratory, Massachusetts Institute of Technology, Cambridge, MA 02139

MAVROMOUSTAKOS, T., D.-P. YANG, W. BRODERICK, D. FOURNIER AND A. MAKRIYANNIS. *Small angle x-ray diffraction studies on the topography of cannabinoids in synaptic plasma membranes.* PHARMACOL BIOCHEM BEHAV **40**(3) 547–552, 1991.—In a previous publication, we have described in detail how we used small angle x-ray diffraction to determine the topography of (−)-Δ^8-tetrahydrocannabinol (Δ^8-THC) in dimyristoylphophatidylcholine (DMPC) bilayers, and to deduce the conformation of the THC side chain by using the iodo-analog (5′-I-Δ^8-THC) in the model membrane. We have now extended our studies to synaptic plasma membrane systems where the cannabinoids are believed to exert part of their pharmacological effects. Synaptic plasma membranes (SPM) were isolated from fresh bovine brains and Δ^8-THC was incorporated into the membranes. By comparing the electron density profiles of drug free and drug-containing SPM preparations, we observed an electron density increase due to the presence of Δ^8-THC in a region centered at 9.2 Å from the terminal methyl groups of the membrane bilayer. In an attempt to dissect the effects of different membrane components on the topography of Δ^8-THC, we carried out parallel experiments using membrane preparations from the synaptosomal membrane total lipid extract (TLX) as well as from bovine brain phosphatidyl choline extract (PCX) containing 30 mole percent cholesterol (Chol). Our results regarding the topography of Δ^8-THC and 5′-I-Δ^8-THC in these lipid membranes show that the TLX bilayer simulates the natural membrane environment very closely whereas in the PCX/Chol bilayer Δ^8-THC resides at a location approximately 4 Å closer to the membrane interface, similar to that found in our previous study using DMPC model membrane. These x-ray diffraction results provide insights regarding the location of the binding sites on the cannabinoid receptor and indicate that preparations of the total lipid extract from synaptosomal membranes duplicate very well the properties of the intact membrane preparation.

X-ray diffraction Cannabinoid Tetrahydrocannabinol Membrane interaction Synaptic plasma membrane

EXISTING evidence shows that many pharmacological actions of cannabinoids can be related to their known effects on biological membranes (8,13). Because of their lipophilic properties, cannabinoids are expected to partition preferentially in the membrane lipids and then diffuse through the bilayer to reach their specific site(s) of action. It has been suggested (6) that the location and orientation of the drug in the bilayer is critical to its ability to interact productively with the active site on the membrane-associated protein. Small angle x-ray diffraction studies on membrane preparations can provide information on the location of the drug in the bilayer, and thus provide us with insights on the corresponding topography of the receptor active site. In our previous work using small angle x-ray diffraction (15), we have determined the location of the biologically active (−)-Δ^8-tetrahydrocannabinol (Δ^8-THC) in a partially dehydrated model membrane from dimyristoylphosphatidylcholine (DMPC) and determined the conformation of the THC alkyl side chain by using an iodinated analog 5′-I-Δ^8-THC (Fig. 1). This method was also used in topographic studies of cannabinoids in several model membranes constructed from a variety of phospholipids, including saturated and unsaturated phosphatidylcholines, and sphingomyelin (14). In order to obtain coherent Bragg-like diffractions at reasonable resolution, the membrane preparation was partially dehydrated by suspending in relative humidity controlled containers, which results in a stack of lamellar lipid bilayers with a definite periodicity. The total period repeat distance (*d*-spacing) can be calculated directly from the observed peaks in the diffraction pattern, and Fourier transformation of the integrated peak intensities gives the electron density profile in the dimension perpendicular to the bilayer (5). When properly normalized and superimposed, the profile from a drug containing bilayer can be compared with that from a control. In such an experiment, the electron density difference will represent the average location of the drug in a specific region of the bilayer.

We have now studied the topography of Δ^8-THC in synaptic plasma membranes (SPM) isolated from fresh bovine brains. To

[1]Requests for reprints should be addressed to Dr. D. P. Yang, School of Pharmacy, U-92, University of Connecticut, Storrs, CT 06269.

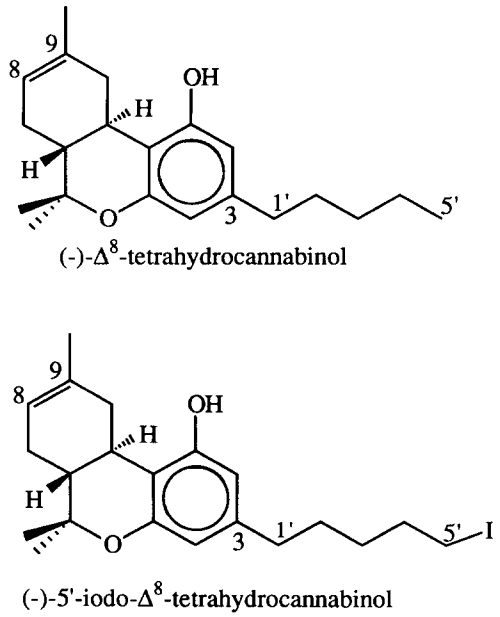

FIG. 1. Structures of Δ^8-THC and 5'-I-Δ^8-THC.

gain a better understanding on how the different components influence the location of the cannabinoid in the bilayer, we have also carried out parallel studies using two lipid membranes in which the membrane proteins are absent. One preparation is from synaptosomal membrane total lipid extract (TLX) which contains all the SPM lipids including phosphatidylcholines, phosphatidylethanolamines, phosphatidylinositol, sphingomyelin and cholesterol. The other preparation is from bovine brain phosphatidyl choline extract (PCX) and consists exclusively of phosphatidylcholines into which cholesterol (Chol) was incorporated at a lipid-to-cholesterol molar ratio 70:30 or $x=0.30$.

By using Δ^8-THC and 5'-I-Δ^8-THC in these two membrane preparations, we were able to obtain information on the topography of the tricyclic cannabinoid components as well as on the conformational preference of the side chain.

METHOD

Materials

Bovine brain was obtained from the local abattoir (Home Pride, Provisions, Inc., Stafford Springs, CT). The cortical synaptosomal membrane preparation was isolated following the method of Cotman and Matthews (2) as modified by Maguire and Druse (10). Protein content for SPM preparation was determined by the method of Lowry et al. (9) and the amount of membrane lipid was calculated based on protein-to-lipid ratio of 1:1 (17). The total lipid extract was obtained from a cortical synaptosomal membrane preparation using the method of Folch (3). Cholesterol was obtained from Sigma Chemical Company (St. Louis, MO) and bovine brain phosphatidylcholine-extract was purchased from Avanti Polar Lipids (Birmingham, AL). According to the chromatographic data provided by the company, the extract was composed of a variety of saturated (14:0, 16:0, 18:0, 20:0, 24:0) and unsaturated (18:3, 20:4, 22:1, 22:6, 24:1) phosphatidylcholines. The major component (18:0) constituted 52% of the composition. Δ^8-THC and 5'-I-Δ^8-THC were synthesized in our laboratory (1).

Methods

Isolation of synaptosomal fraction. Bovine brain was removed from the cranium in the cold and the entire brain immediately placed in cold isolation medium (0.32 M sucrose, 10 mM Tris, 5 mM EDTA, pH 7.4). The temperature was kept at 4°C for all the subsequent steps and all the reagents. The cerebral cortex was dissected from the brain and the meninges removed. The cortical tissue was homogenized in cold isolation medium at a ratio of 1:5 (tissue:buffer) with a hand held Potter Elvehjem glass/glass homogenizer using 12 strokes. The homogenate was centrifuged (Beckman 52-21) at $1,100\times g$ for 15 min. The supernatant fraction was recentrifuged at $11,000\times g$ for 20 min. The resultant pellet was resuspended in isolation medium at a ratio of 1:2 (pellet:isolation medium). Homogenate aliquots of 1.2 ml were mixed gently with 6 ml of 14% (w/v) Ficoll solution. This suspension was layered with 3 ml of 6.0% (w/v) Ficoll solution and tubes topped with isolation medium. The discontinuous gradients were centrifuged (Beckman L8-55 ultracentrifuge, SW 40 swinging bucket rotor) at $99,000\times g$ for 30 min with the brake off. Myelin formed a fluffy white layer at the interface of the isolation medium and 6.0% Ficoll layer. The synaptosomal fraction formed a band at the interface of the 6.0% and 14% Ficoll solution layers. Mitochondria formed a pellet at the bottom of the tube.

Isolation of synaptic plasma membranes. Synaptic plasma membranes (SPM) were prepared from the above synaptosomal fraction. Briefly, the synaptosomal fraction collected from the Ficoll gradient was washed with 8.0 ml isolation medium, mixed using a Vortex mixer then centrifuged (Beckman L8-55 ultracentrifuge, Type 65 rotor) at $78,000\times g$ for 30 min. The resultant pellet was resuspended and homogenized in 8 ml of isolation medium. The synaptosomes were osmotically lysed with the addition of 40 ml of 6 mM Tris-HCl (pH 8.1) followed by incubation on ice for 90 min. The lysed synaptosomes were centrifuged at $54,000\times g$ for 15 min. The pellet was resuspended and homogenized in 0.3 M sucrose. The suspension was layered on a discontinuous sucrose gradient of 0.6 M and 1.0 M sucrose (2.5 ml each step). The tubes were centrifuged (Type SW 40 rotor) at $63,500\times g$ for 90 min. The SPM band at the 0.6 M/1.0 M sucrose interface was recentrifuged (Type 65 rotor) at $78,000\times g$ for 30 min. The pellet was kept in 10 mM Tris-HCl (pH 7.4) and used for small angle x-ray diffraction sample preparation.

Total lipid extract of synaptic plasma membranes. SPM prepared as above were homogenized in Kreb-Henseleit buffer (pH 7.4) (1:1) containing 0.1% ascorbate using a Ten Broeck tissue homogenizer (0.15 mm clearance). Serial methanol-chloroform extractions of SPM at room temperature yielded a total lipid extract. The final lower phase containing the lipid extract was evaporated to dryness under a stream of nitrogen in a water bath at 40°C. The residue was redissolved in chloroform:methanol (2:1), filtered (Buchner funnel with fritted disc) and stored under nitrogen at −20°C.

Small angle x-ray diffraction sample preparation. Each x-ray sample from SPM preparation containing the equivalent of 5 mg of dry lipid was diluted to 1 ml with isolation buffer (0.32 M sucrose, 10 mM Tris, 5 mM EDTA, pH 7.4) and 2 μl of the cannabinoid solution in ethanol was then added while the membrane suspension was being gently vortexed. The drug concentration was 6.5 μM or the lipid-to-drug molar ratio was 95:5. For the control membrane sample, 2 μl of pure ethanol was added. After incubation at 37°C for 1 h, the suspension was centrifuged for 1 h at 4°C in clear, lucite sedimentation cells (7) and spun

down on an aluminum foil substrate using swinging bucket SW28 rotor at 25000 rpm (81000 × g) in a Beckman L8-55 ultracentrifuge. The supernatant was then removed using a pipet. Lipid extracts (TLX or PCX/Chol) were prepared by dissolving 1 mg of lipid and the appropriate amount of drug in 0.25 ml $CHCl_3$. The solution was then dried under a stream of O_2-free N_2 gas at 50°C and placed under vacuum (0.1 mmHg) for 6 h at 20°C. To the residue was added 250 μl of distilled water and it was well mixed by vortexing and bath sonicated for 15 min at 50°C. The translucent suspension was deposited on an aluminum foil and allowed to dry at room temperature. All the membrane samples on aluminum foils were mounted on curved glass holders and equilibrated by suspending over a saturated K_2SO_4 solution to maintain a relative humidity (RH) of 98%.

X-ray diffraction instrumentation. The small angle x-ray diffraction experiments were carried out with an Elliott GX18 generator supplying CuKα radiation ($\lambda = 1.54$ Å) with a camera utilizing a single vertical Franks' mirror (4). Small angle x-ray diffraction patterns were collected using a Braun position sensitive proportional counting gas flow detector which has an average of 29.28 channels per mm in the dimension of the diffraction. During the experiment, we used a helium path for a specimen-to-detector distance of 170 mm and collected the diffraction data with digital accumulations of 1×10^6 to 2×10^6 counts to improve the signal-to-noise ratio. Data was transferred to a VAX computer system and the intensities were integrated directly from the computer graphics by calculating the area under the diffraction peaks.

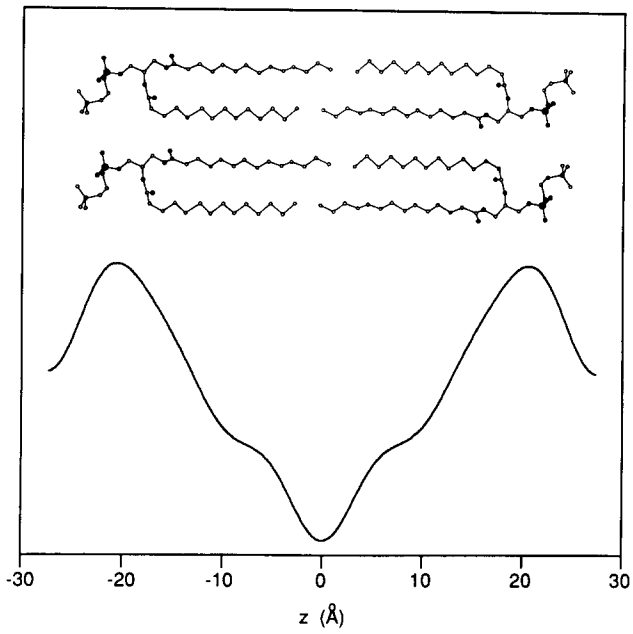

FIG. 2. Electron density profiles obtained by Fourier transform of small angle diffraction intensities for DMPC at 22°C equilibrated at RH 98%. A molecular graphic representation of DMPC bilayer above the electron density profile shows the space correlation in the dimension across the bilayer.

RESULTS

From each diffraction patter, the *d*-spacing of the membrane preparation was calculated using Bragg's law $2d \sin \theta = h\lambda$ where θ is the diffraction angle. Typically bilayer preparations showed *d*-spacings of 55–60 Å corresponding to the length of two lipid molecules. The diffraction patterns were considered centrosymmetric, and allowed us to derive the corresponding electron density profile in the dimension *z* across the bilayer through Fourier transformation. Whenever possible, the experimentally determined relative electron density was converted to profiles with an absolute scale using the step-function approach described earlier in detail (15,18). Figure 2 shows a typical electron density profile of a DMPC bilayer equilibrated at RH 98% at 22°C. A molecular graphical representation of the bilayer is shown above the electron density profile to scale. The maximum electron density at $z = \pm 20$ Å corresponds to the phospholipid head group and the minimum at $z = 0$ to the terminal methyl group region. When comparing electron density profiles between the drug free and drug-containing preparations, we sought to ensure that both preparations had the same mesomorphic state. Earlier experimental data had localized Δ^8-THC near the bilayer interface (11). The two profiles were then superimposed after normalizing at the phosphate and the terminal methyl groups as we described elsewhere (15).

A comparison of the electron density profiles from membrane preparations without and with drug molecule gives information on the location of the drug as well as on the conformational changes in the bilayer due to the presence of the drug. In the preparation with the halogenated analog, the iodine atom, because of its high electron density, serves as a probe and provides information on the conformational behavior of the side chain. The procedures were described in detail in our previous publication (15).

Figure 3 shows the diffraction patterns of SPM preparations without (A, C) and with Δ^8-THC ($x = 0.05$; B, D) at 9°C and RH 98% at two different dehydration stages. Patterns A and B were obtained during the initial dehydration period, typically within 12 h, and each showed two Bragg-like diffraction peaks ($h = 1$ and $h = 2$) and a very broad diffraction band to the left of the 2nd order peak. We were also able to observe the $h = -1$ peak on the opposite side of the incident beam and used the $h = 1$ and $h = -1$ peaks to calculate the *d*-spacing values accurately, which were both 69.0 Å for the drug free and drug-containing SPM preparations. Pattern B showed a noticeable improvement in the sharpness of the 2nd order peak, probably indicating an ordering effect by the cannabinoid in the synaptic plasma membrane. Upon further dehydration (typically after 24 h), the preparations changed into a more stable state which showed six orders of diffraction with a *d*-spacing of 57.38 Å for the drug-free preparation (Pattern C) and 57.98 Å for the drug-containing preparation (Pattern D). The change in the *d*-spacing values of the SPM samples from the initial dehydration to the final state was 12 Å and was always accompanied by an improvement in the sharpness of the diffraction peaks.

From the integrated intensities of the diffraction peaks in Patterns C and D, we have derived the electron density profiles and superimposed them in Fig. 4. The head groups (electron density maxima) occur at $z = \pm 23.2$ Å. Inspecting the profiles inside the bilayer (-23.2 Å$< z < +23.2$ Å) we notice that the one representing SPM + Δ^8-THC had an elevated electron density near $z = \pm 9.2$ Å on each side of the bilayer. To view this difference more clearly and quantitatively, we have subtracted Profile C from Profile D and plotted the difference with a 2.5 times expanded scale at the bottom of Fig. 4. The net increase in electron density indicates that Δ^8-THC incorporates in the bilayers of synaptic plasma membrane. The increase, which can be attributed to the presence of the cannabinoid in this location

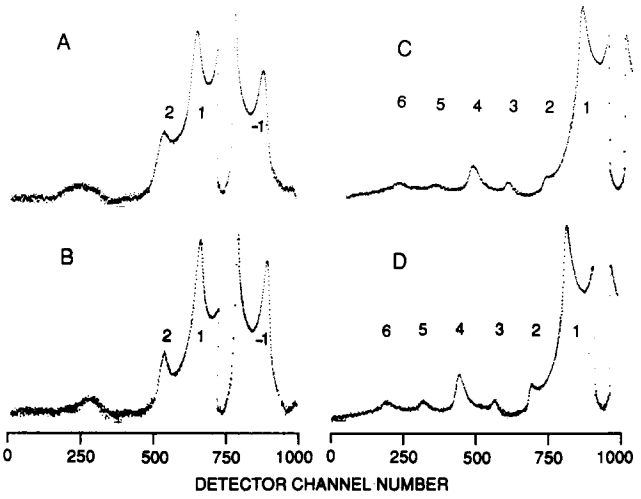

FIG. 3. Diffraction patterns of SPM preparations at 9°C and equilibrated at RH 98%. Initial dehydration: (A) SPM and (B) SPM + Δ^8-THC; Further dehydration: (C) SPM and (D) SPM + Δ^8-THC.

of the bilayer, is centered at $z = \pm 9.2$ Å and had the familiar Gaussian-type distribution extending to a half-height width of $\Delta z = 5$ Å.

Parallel x-ray diffraction experiments using TLX and PCX/Chol preparations showed that these reconstituted lipid membranes always provided six very sharp orders of diffraction which were similar to those observed with preparations from a single phospholipid (14). The presence of Δ^8-THC or 5′-I-Δ^8-THC did not produce any qualitative changes in the diffraction pattern, indicating that the drug molecules had not altered the mesomorphic state of the preparations. Analysis of the peak intensities revealed that the drug-containing bilayers had increased electron densities in the hydrocarbon core.

Figure 5 shows the superimposed electron density profiles

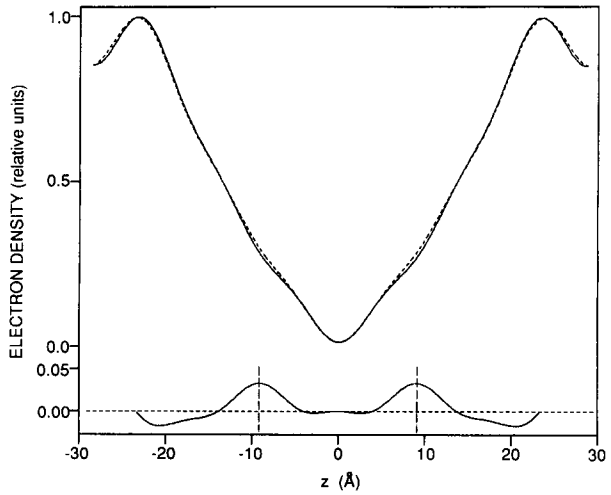

FIG. 4. Above: Superimposed electron density profiles (A) SPM (solid line) and (B) SPM + Δ^8-THC (short dashed line) at 9°C and equilibrated at RH 98%. Below: Electron density profile difference inside the bilayer between SPM and SPM + Δ^8-THC. The vertical dashed lines indicate the peaks in the difference and represent the position of the tricyclic component of Δ^8-THC in the bilayer.

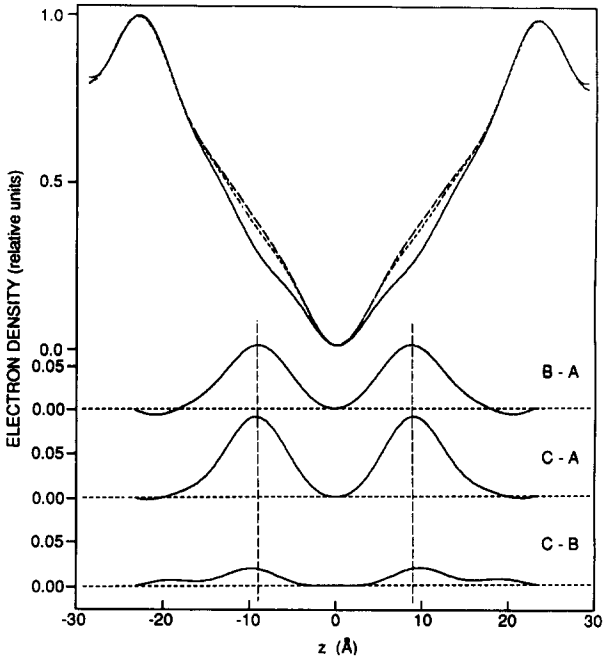

FIG. 5. Above: Superimposed electron density profiles of (A) TLX (solid line), (B) TLX + Δ^8-THC (short dashed line) and (C) TLX + 5′-I-Δ^8-THC (long dashed line) at 9°C and equilibrated at RH 98%. Below: Electron density profile differences inside the bilayer. (B − A) difference between Profiles B and A, (C − A) difference between Profiles C and A, and (C − B) difference between Profiles C and B. The vertical dashed lines indicate the peaks in these difference curves and represent the positions of the tricyclic component of Δ^8-THC as well as the iodine atom of 5′-I-Δ^8-THC in the bilayer.

of (A) TLX, (B) TLX + Δ^8-THC ($x = 0.15$) and (C) TLX + 5′-I-Δ^8-THC ($x = 0.15$) at 9°C. The d-spacing values were 57.39 Å, 58.14 Å and 58.14 Å, respectively, both drug-containing membranes having d-spacing values almost 1 Å larger than the control preparation. Pronounced differences between these profiles were visible in the bilayer region of $z = \pm 9.2$ Å, which coincides the location of Δ^8-THC in the natural synaptic plasma membrane. As expected, the preparation containing 5′-I-Δ^8-THC with the heavy atom iodine-label showed a linear increase in electron density. We found that this increase, due to the iodine atom, was quantitatively consistent with the increase due to the rest of the drug molecule on the basis of total number of electrons in each atom of the drug. In the lower part of Fig. 5, three electron density differences, B-A, C-A and C-B, with a 2.5 times expanded scale show the distribution of the electron density increases due to the presence of Δ^8-THC, 5′-I-Δ^8-THC and the iodine atom, respectively. Difference B-A shows that Δ^8-THC is located at 9.2 Å from the center of the bilayer, while Difference C-B shows a net increase due to the iodine atom which is also centered at $z = \pm 9.2$ Å.

The results with lipid membranes from bovine brain lipid-extract which contain only phosphatidyl cholines and cholesterol, PCX/Chol, PCX/Chol + Δ^8-THC ($x = 0.15$) and PCX/Chol + 5′-I-Δ^8-THC ($x = 0.15$), are shown in Fig. 6. At 9°C, the d-spacing values of the three preparations were 54.28 Å, 53.40 Å and 53.25 Å, respectively. Contrary to the case of TLX, both drug-containing preparations had d-spacing values 1 Å smaller than the control. Also, the increases in electron density between profiles were now located in different regions. The expanded electron density differences in the lower part of Fig. 6 show that

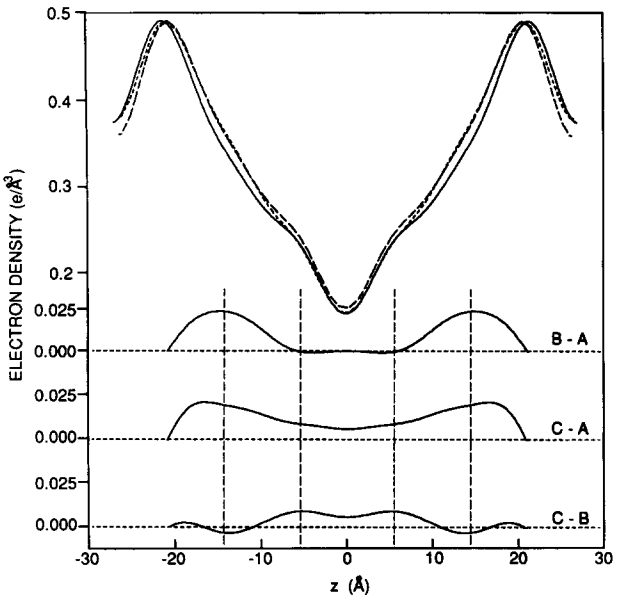

FIG. 6. Above: Superimposed electron density profiles of (A) PCX/Chol (solid line), (B) PCX/Chol + Δ^8-THC (short dashed line) and (C) PCX/Chol + 5′-I-Δ^8-THC (long dashed line) at 9°C and equilibrated at RH 98%. Below: Electron density profile differences inside the bilayer. (B − A) difference between Profiles B and A, (C − A) difference between Profiles C and A, and (C − B) difference between Profiles C and B. The outer pair of the vertical dashed lines indicates the peaks in curve B − A and the inner pair indicates the peaks in C − B. They represent the positions of the tricyclic component of Δ^8-THC and the iodine atom of 5′-I-Δ^8-THC in the bilayer, respectively.

the tricyclic ring system of Δ^8-THC is located at $z = \pm 14$ Å while the iodine label is localized at $z = 5.5$ Å.

The relative amounts of electron density increases due to the presence of Δ^8-THC in these three different membrane preparations show that the TLX preparation can accommodate the largest amount of Δ^8-THC, and we estimated that the lipid-to-Δ^8-THC molar ratio in SPM was approximately 99:1.

DISCUSSION AND CONCLUSIONS

The *d*-spacing values indicate that in all of the membrane preparations, the lipids exist in the liquid crystalline phase. During the initial dehydration period, the SPM preparations showed distinct relatively broad Bragg-like 1st and 2nd order diffractions. These orders represent a bilayer structure with a thickness of almost 70 Å similar to that observed in intact brain synaptoneurosome (16). When Δ^8-THC is added in micromolar amounts to the SPM preparation, the resulting diffraction pattern shows a sharper 2nd order peak, indicating that the drug has an ordering effect on the bilayer.

Longer equilibration times at RH 98% produce a striking change in the diffraction pattern of the SPM preparation. The *d*-spacing decreases from 69 Å to 57 Å and the sample shows six diffraction orders which appear as relatively sharp peaks, similar to those observed in lipid membranes. This transformation, which involves a decrease in *d*-spacing accompanied by a higher degree of ordering in the membrane, may be due to the formation of two different domains, one being rich in lipid and the other rich in protein. In all likelihood, the diffraction pattern observed is therefore mainly due to the lipid enriched domains. This view is strongly supported by the similarity of these diffraction patterns with those observed in TLX, PCX and synthetic lipid bilayers.

The observation of six well-defined diffraction orders from SPM preparations allowed us to derive the electron density profiles of drug free and Δ^8-THC-containing bilayers. The comparison revealed a small electron density increase, yet large enough to identify the location of Δ^8-THC in the hydrocarbon core region of the membrane. Interestingly, in this SPM preparation, Δ^8-THC is located approximately 2–5 Å deeper in the bilayer than in the corresponding DMPC bilayer system.

We found that in the total lipid extract from SPM, Δ^8-THC occupies the same location as in the intact SPM. This points out that this reconstituted lipid membrane can serve as an excellent model for the intact membrane when studying the topography of cannabinoids in brain membrane. Furthermore, the data indicate that, when in the intact membrane, at least the major fraction of the cannabinoids interact with the lipid component of the membrane.

The use of an iodine label in 5′-I-Δ^8-THC allowed us to obtain information regarding the conformation of the cannabinoid side chain in the TLX bilayers. Unlike our previous results with DMPC bilayers, the iodine atom is now located at the same depth as the tricyclic component.

In contrast with the cases of SPM and TLX, the results from the PCX/Chol preparations show that the tricyclic component of Δ^8-THC and the iodine atom are located at 14.4 Å and 5.5 Å, respectively, from the center of the bilayer. These results are almost identical to those found with the DMPC bilayers (18). It is, thus, likely that the topography of Δ^8-THC in PCX/Chol bilayers is the same as in DMPC bilayers where the phenolic hydroxy group of Δ^8-THC is near the bilayer interface between the polar head group and the hydrophobic acyl chains. Earlier work from our laboratory using solid state ^{2}H-NMR showed that Δ^8-THC orients with the long axis of its tricyclic component perpendicular to the lipid chains (11). The location of the iodine atom of 5′-I-Δ^8-THC requires the cannabinoid five-membered chain to orient towards the center of the bilayer and be parallel to the lipid chains. This can be achieved by invoking one *gauche* methylene conformer around the $C_{1'}$-$C_{2'}$ bond followed by two *trans* conformers around $C_{2'}$-$C_{3'}$ and $C_{3'}$-$C_{4'}$ bonds. In such a conformation the five methylene carbon chain runs parallel with the lipid bilayer chains and does not contribute to the overall electron density profile.

One interpretation of the above findings is that in the SPM and TLX preparations, the cannabinoid side chain assumes a conformation which positions the iodine atom at approximately the same level as the tricyclic ring system. This can be accomplished through a *g-t-g* conformation around the $C_{1'}$-$C_{2'}$, $C_{2'}$-$C_{3'}$, and $C_{3'}$-$C_{4'}$ bonds, respectively. Such a conformation will allow the 5′-I-Δ^8-THC side chain to be fully accommodated within the same bilayer leaflet and does not require interdigitation with the other leaflet. We expect that while in this more compact conformation, the five methylene units will contribute to the increase in electron density in the bilayer profile along with the tricyclic system. The molecular modelling (see Fig. 7) used to interpret the net increases in electron density due to the drug finds the cannabinoid approximately 2–3Å deeper in the bilayer than in our previous experiments (11), and positions the phenolic OH somewhat below the *sn*-1 carbonyl. Such a model will still allow two successive hydrogen bondings between the phenolic OH water and *sn*-1 carbonyl. It appears that the conformational differences between the cannabinoid side chains in the different membrane preparations are dictated by the depth at which the cannabinoid tricyclic system localizes. In the case of membranes composed entirely of lipids with phosphocholine head groups, with or without cholesterol, the drug resides near the bilayer in-

terface and allows the five-carbon cannabinoid side chain to assume a more extended conformation. Conversely, in the intact membrane, or in lipid membranes composed of phospholipids with other types of head groups such as phosphoethanolamines and phosphoserines, the drug location is 2–3 Å deeper in the bilayer and forces the cannabinoid side chain into a more compact conformation.

An examination of the changes in *d*-spacings resulting from the presence of the cannabinoid in the bilayers shows that the location of the drug may also influence its effects on the bilayer conformation and dynamics. In both SPM and TLX preparations, the Δ^8-THC increases the bilayer *d*-spacing by 1 Å indicating an increase in the order of the chains. Conversely, in the PCX/Chol preparation, the drug produces a decrease of 1 Å in the bilayer thickness indicating some bilayer perturbation. This is in agreement with earlier work from our laboratory in which we demonstrated that membrane perturbation by a ligand is most effective when the drug-membrane interaction occurs at or near the interface.

The work presented here demonstrates that the membrane composition may determine the location of the drug in the membrane. A similar observation with cardiac membranes has also been recently reported (12). At this stage, it is difficult to assess the implications of our data regarding the cannabinoid mode of action. However, it is tempting to speculate that the variations in cannabinoid topography depending on membrane composition as described in this publication may help explain the tissue selectivity observed with cannabinoids. Currently, we are further pursuing this line of research.

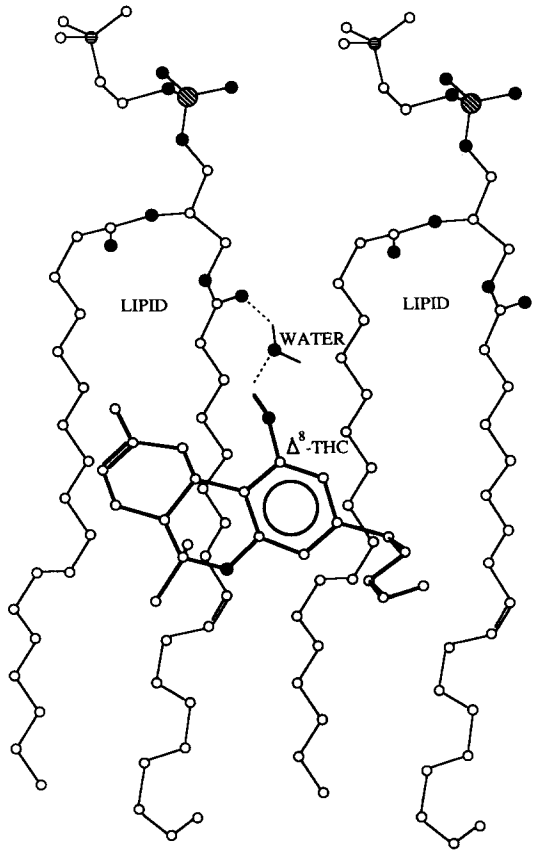

FIG. 7. Graphical representation of the topography of 5′-I-Δ^8-THC in TLX and SPM.

ACKNOWLEDGEMENTS

This work was supported by grants from the National Institute on Drug Abuse (DA-3801) and the University of Connecticut Research Foundation (UCRF-35491). The x-ray diffraction experiments were carried out in the Biomolecular Structure Analysis Center at the University of Connecticut Health Center. We are grateful to its personnel and especially Professor Leo Herbette for making their facilities available to us. We are also thankful to Avgui Charalambous for the synthesis of 5′-I-Δ^8-THC.

REFERENCES

1. Charalambous, A.; Lin, S.; Marciniak, G.; Banijamali, A.; Friend, F. L.; Compton, D. R.; Martin, B. R.; Makriyannis, A. Pharmacological evaluation of halogenated Δ^8-THC analogs. Pharmacol. Biochem. Behav. 40:509–512; 1991.
2. Cotman, C. W.; Matthews, D. A. Synaptic plasma membranes from rat brain synaptosomes: Isolation and partial characterization. Biochim. Biophys. Acta 249:380–394; 1971.
3. Folch, J.; Lees, M.; Stanley, S. A simple method for the isolation and purification of total lipides from animal tissues. J. Biol. Chem. 226:497–509; 1957.
4. Franks, A. X-ray optics. Sci. Prog. Oxf. 64:371–422; 1977.
5. Franks, N. P.; Levine, Y. K. In: Grell, E., ed. Membrane spectroscopy. New York: Springer-Verlag; 1981:437–487.
6. Herbette, L. G.; Chester, D. W.; Rhodes, D. G. Structural analysis of drug molecules in biological membranes. Biophys. J. 49:91–96; 1986.
7. Herbette, L. G.; Marquardt, J.; Scarpa, A.; Blasie, J. K. A direct analysis of lamellar X-ray diffraction from hydrated oriented multilayers of fully functional sarcoplasmic reticulum. Biophys. J. 20: 245–272; 1977.
8. Hillard, C. J.; Pounds, J. J.; Boyer, D. R.; Bloom, A. S. Studies of the role of membrane lipid order in the effects of Δ^9-tetrahydrocannabinol on adenylate cyclase activation in heart. J. Pharmacol. Exp. Ther. 252(3):1075–1082; 1990.
9. Lowry, O. H.; Rosebrough, N. J.; Farr, L. A.; Randall, R. J. Protein measurement with the folin phenol reagent. J. Biol. Chem. 193:265–275; 1951.
10. Maguire, P. A.; Druse, M. J. The influence of cholesterol on synaptic fluidity, dopamine D_1 binding and dopamine-stimulated adenylate cyclase. Brain Res. Bull. 23:69–74; 1989.
11. Makriyannis, A.; Yang, D. P. In: Hondeghem, L., ed. Molecular and cellular mechanisms of antiarrhythmic agents. Mount Kisco, NY: Futura Publishing Co.; 1989:293–305.
12. Mason, R. P.; Moring, J.; Herbette, L. G. In: Makriyannis, A., ed. New methods in drug research. vol. 4. Barcelona, Spain: Prous Science Publishers; 1991: in press.
13. Matsuda, L. A.; Lolait, J. S.; Brownstein, M. J.; Young, A. C.; Bonner, T. I. Structure of a cannabinoid receptor and functional expression of the clone cDNA. Nature 346:561–564; 1990.
14. Mavromoustakos, T. Cannabinoid and anesthetic steroid interactions with membranes. Ph.D. dissertation. University of Connecticut. 1990.
15. Mavromoustakos, T.; Yang, D. P.; Charalambous, A.; Herbette, L. G.; Makriyannis, A. Study of the topography of cannabinoids in model membranes using X-ray diffraction. Biochim. Biophys. Acta 1024:336–344; 1990.
16. Moring, J.; Shoemaker, W. J.; Mason, R. P.; Hayden, H. C.; Salomon, R. M.; Herbette, L. G. Rat cerebral cortical synaptoneurosomal membranes. Structure and interaction with imidazobenzodiazepine and 1,4-dihydropyridine calcium channel drugs. Biophys. J. 58:513–531; 1990.
17. Smith, A. P.; Loh, H. H. Architecture of the nerve ending membrane. Life Sci. 24:1–20; 1979.
18. Worthington, C. R. The interpretation of low-angle x-ray data from planar and concentric multilayered structures, the use of one-dimensional electron density strip models. Biophys. J. 9:222–234; 1969.